Journal of General Virology (2002), **83**, 2869–2877. Printed in Great Britain

Nucleotide sequence and genomic organization of an ophiovirus associated with lettuce big-vein disease

F. van der Wilk,[1] A. M. Dullemans,[1] M. Verbeek[1] and J. F. J. M. van den Heuvel[2]

[1] Plant Research International BV, PO Box 16, 6700 AA Wageningen, The Netherlands

[2] De Ruiter Seeds, PO Box 1050, 2660 BB Bergschenhoek, The Netherlands

The complete nucleotide sequence of an ophiovirus associated with lettuce big-vein disease has been elucidated. The genome consisted of four RNA molecules of approximately 7·8, 1·7, 1·5 and 1·4 kb. Virus particles were shown to contain nearly equimolar amounts of RNA molecules of both polarities. The 5′- and 3′-terminal ends of the RNA molecules are largely, but not perfectly, complementary to each other. The virus genome contains seven open reading frames. Database searches with the putative viral products revealed homologies with the RNA-dependent RNA polymerases of rhabdoviruses and *Ranunculus white mottle virus*, and the capsid protein of *Citrus psorosis virus*. The gene encoding the viral polymerase appears to be located on the RNA segment 1, while the nucleocapsid protein is encoded by the RNA3. No significant sequence similarities were observed with other viral proteins. In spite of the morphological resemblance with species in the genus *Tenuivirus*, the ophioviruses appear not to be evolutionary closely related to this genus nor any other viral genus.

Introduction

Lettuce big-vein disease (BVD) is the most serious fungus-transmitted virus disease of lettuce and other leafy vegetables. The disease occurs in all major lettuce-producing areas. The causal agent of big-vein disease is transmitted by the common, soil-borne, root-infecting fungus *Olpidium brassicae* (Campbell, 1962). The disease is particularly difficult to control since the resting spores of the fungus can persist for over 20 years in soil and can retain the ability to transmit the disease for over 15 years, making eradication extremely difficult, if not impossible. Moreover, major resistance genes are not available in commercial varieties of lettuce and other leafy vegetables.

A complex of two viruses appears to be associated with big-vein disease. Rod-shaped particles have been identified in infected plants and an antiserum has been raised against these particles (Kuwata *et al.*, 1983; Vetten *et al.*, 1987; Huijberts *et al.*, 1990). They contained negative-sense single-stranded RNA and are serologically related to *Tobacco stunt virus* (TStV) (Kuwata *et al.*, 1983; Sasaya *et al.*, 2001). Since it was generally believed that this virus was the causal agent of big-vein disease the virus was named *Lettuce big-vein virus* (LBVV) (Kuwata *et al.*, 1983; Huijberts *et al.*, 1990). Based upon serological relationship, morphology and partial sequence analysis of the coat protein gene (Sasaya *et al.*, 2001) LBVV was classified as the type member of the genus *Varicosavirus* (Mayo, 2000). However, no evidence was obtained that infection with LBVV induced big-vein symptoms in lettuce.

Recently, a second virus has been isolated from lettuce plants showing big-vein symptoms (Roggero *et al.*, 2000). The particles of the virus morphologically resembled those of the ophioviruses and the virus was reported to be serologically related to the ophiovirus *Ranunculus white mottle virus* (RWMV) The authors tentatively named it Mirafiori lettuce virus (MiLV). Lot *et al.* (2002) reported that an infection with MiLV alone was sufficient to induce big-vein-like symptoms in lettuce, while plants infected with LBVV remained symptomless, suggesting that MiLV was the causal agent of big-vein disease.

Species in the genus *Ophiovirus* have filamentous virus particles resembling those of the tenuiviruses. The ophiovirus ribonucleoprotein particles are pleiomorphic. Electron microscopical analysis revealed that the particles appear as thin filamentous either collapsed double-stranded forms of circular particles of 3 nm in diameter or as linear spiral filaments of 10 nm in diameter (Barthe *et al.*, 1998; Milne *et al.*, 2000). The viruses are believed to have both small and large particles,

Author for correspondence: Frank van der Wilk. Present address: COGEM, PO Box 578, 3720 AN Bilthoven, The Netherlands. Fax +31 30 2744461. e-mail Frank.van.der.Wilk@RIVM.nl

possibly due to encapsidation of RNA molecules of different sizes (Barthe *et al.*, 1998; de la Torre *et al.*, 1998). The genome of ophioviruses is multipartite and consists of three single-stranded (ss) negative-sense RNA molecules of approximately 1·5, 1·6–1·8 and 7·5–9 kb in size (Milne *et al.*, 2000). The capsid proteins of the ophioviruses have reported sizes ranging between 40 and 50 kDa.

Molecular data are lacking for this virus genus. Only partial sequence data are available for RWMV and *Citrus psorosis virus* (CPsV; Barthe *et al.*, 1998; de la Torre *et al.*, 1998). The absence of sequence data impedes our understanding of the molecular biology of the ophioviruses and their taxonomic relationships with the tenuiviruses or other possibly related viruses like the *Bunyaviridae*. In this paper, we report the nucleotide sequence of MiLV. This is the first report of a complete nucleotide sequence of an ophiovirus. Unexpectedly, the genome of MiLV consisted of four RNA molecules, ranging between 7·8 and 1·4 kb in size.

Methods

■ **Virus isolates and purification.** A lettuce plant showing symptoms characteristic of lettuce big-vein disease (isolate LS301) was a kind gift of J. Schut (Rijk Zwaan, the Netherlands). An ophiovirus (virus strain LS301-O) was transferred from this plant by mechanical inoculation and maintained in *Nicotiana hesperis* 'P1' (M. Verbeek and others, unpublished). Infectious virus particles were isolated from infected plant material by homogenizing 100 g of leaves in 5 vols of homogenization buffer (0·1 M Tris–HCl, pH 8, 20 mM Na_2SO_3, 10 mM Na-DIECA and 5 mM Na-EDTA) in a Waring blender. The homogenate was filtered through cheese cloth and clarified by centrifugation at 49000 ***g*** for 30 min. Subsequently, the supernatant was layered on a 20% sucrose cushion (20% sucrose in homogenization buffer) and centrifuged at 96000 ***g*** for 3 h. The pellets were suspended in 100 ml homogenization buffer and the virus was precipitated from the suspension by addition of PEG 6000 and NaCl to final concentrations of 6% and 0·5%, respectively. The suspension was stirred for 1 h, allowed to settle for 1 h and centrifuged at 23500 ***g*** for 20 min. The precipitate was resuspended in 40 ml homogenization buffer by gentle stirring for 16 h. After centrifugation (10 min at 13000 ***g***) the supernatant was layered onto a 30% sucrose cushion (in homogenization buffer) and centrifuged for 3 h at 96000 ***g***. The pellets were resuspended in 1 ml 0·1 M Tris–HCl, pH 8 and subjected to equilibrium gradient centrifugation in 10–40% Cs_2SO_4 (in 0·1 M Tris–HCl, pH 8) for 20 h at 40000 r.p.m. in a Beckman SW60 rotor. The virus was then diluted with 0·1 M Tris–HCl, pH 8 and pelleted at 40000 r.p.m. in a Beckman SW55 rotor for 3 h.

■ **cDNA synthesis and cloning.** Genomic RNA was purified from virus particles with a Qiagen RNA Kit (Qiagen), according to the manufacturer's instructions. Synthesis of cDNA was carried out by priming with random hexanucleotide primers, using the SuperScript System II (Life Sciences) according to the supplier's instructions. The double-stranded cDNA fragments were cloned into the Lambda ZAP vector (Stratagene). Identification of recombinant clones and subsequent isolation of plasmid DNA was done following standard procedures (Sambrook *et al.*, 1989).

The 5′- and 3′-terminal ends of the MiLV genomic RNAs were determined using 5′RACE (rapid amplification of cDNA ends) and 3′RACE procedures. The RACE procedures were carried out by RT–PCR using commercially available kits (Life Technologies). The tailing reaction of the cDNA in the 5′RACE procedure was performed using dCTP. In the 3′RACE procedure the genomic RNAs were tailed using ATP and yeast poly(A) polymerase (USB) according to the manufacturer's instructions. The PCR fragments obtained were cloned using the TOPO TA cloning kit (Invitrogen), according to the manufacturer's instructions.

■ **DNA sequencing.** Sequence analysis was performed with an Applied Biosystems model 373 automated sequencer, using a sequencing kit with AmpliTaq DNA polymerase (Applied Biosystems), and universal and MiLV sequence-specific primers. The MiLV genomic sequence was determined from overlapping independent clones. Each nucleotide of the MiLV genome was determined by sequencing at least two different clones. The entire sequence was determined by sequencing both strands of each clone.

To determine whether the presence of two open reading frames (ORFs) on the RNA1 was not specific for isolate LS301-O and conserved among different isolates RT–PCR was carried out to amplify the genomic region of the RNA1 of a Norwegian isolate spanning the intergenic region between these ORFs (position 6520–7273 of the MiLV genome). This isolate has been in the our virus collection since 1987 and was a kind gift of D.-R. Blystad. To confirm the observed frameshift in the reading frame of RNA segment 4, the region spanning the overlapping reading frames (position 134–583 of the vRNA) was amplified by RT–PCR using the genomic RNA of a Norwegian isolate as template, followed by sequencing of the obtained PCR fragments.

■ **Computer analysis.** The nucleotide and protein sequences were compiled, analysed and compared using the Wisconsin Package software [version 9, Genetics Computer Group (GCG), Madison, WI, USA], the DNASTAR Lasergene software package and the BLAST suite (Altschul *et al.*, 1997). Phylogenetic analysis was carried out using ClustalW. The phylogenetic tree was generated using the neighbour-joining method (1000 bootstrap replicates).

■ **SDS–PAGE.** Purified virus suspensions were denatured by boiling in Laemmli buffer (Laemmli, 1970) for 10 min. The samples were loaded onto a 12·5% SDS–polyacrylamide gel and subjected to electrophoresis. After electrophoresis the proteins were visualized by silver staining.

■ **Northern blot analysis.** To detect MiLV-specific sequences, the purified RNA was separated on a denaturing 1% agarose gel containing formaldehyde (Sambrook *et al.*, 1989) and transferred to (positively charged) nylon membranes (Roche). To detect specific strand RNA molecules the blots were probed with DIG-labelled T7 and T3 transcripts of genomic cDNA fragments. To obtain strand-specific transcripts cDNA fragments complementary to regions of the different RNA segments were cloned behind the T7 or T3 promoter: RNA1, nt 3888–4845; RNA2, nt 82–602; RNA3, nt 48–1154; RNA4, nt 17–1188 (positions are indicated on the vRNA). Strand-specific riboprobes used to detect the presence of the different RNA polarities of a specific RNA segment spanned the same genomic region. Labelling of the probes was carried out using the DIG RNA Labelling Kit (Roche) according to the manufacturer's instructions. Detection levels of the different probes were tested, compared and calibrated using cDNA clones as a control. Hybridization and subsequent detection of the trapped probes was carried out employing DIG Easy Hyb, anti-digoxigenin alkaline phosphatase-conjugated Fab fragments and CDP-Star (Roche).

■ **Nucleotide sequence accession numbers.** The nucleotide sequences reported here appear in the EMBL, GenBank and DDBJ nucleotide sequence databases under accession numbers AF525933, AF525934, AF525935 and AF525936.

Results

Purification and characterization of virus particles

Virus particles were isolated from infected *N. hesperis* 'P1' plants. On inoculation on indicator plants (*N. hesperis* 'P1', *Chenopodium quinoa*) the particles were infectious and induced symptoms previously described for MiLV infection. Electron microscopical analysis revealed that the particles were approximately 10 nm in diameter with the characteristic appearance of ophiovirus particles. Purified virus was subjected to SDS–PAGE. On silver-stained gels a major protein of approximately 50 kDa was detected together with a number of minor proteins (Fig. 1). Western blot analysis using infected and non-infected plant material showed that the 50 kDa protein was virus specific (data not shown). The other proteins are possibly co-purified host proteins.

Analysis of the viral genomic material isolated from purified virus particles revealed the presence of four RNA molecules of approximately 1·4, 1·5, 1·6 and 8 kb in length (Fig. 2). Additionally, a small RNA of approximately 200 nucleotides was present on the gel. The nature of this small RNA is unclear; possibly it represents a satellite RNA, or subgenomic mRNA. However, most likely this RNA is the result of degradation of the larger RNA molecules since in other experiments this small RNA was not present as a distinct band but rather as a smear, typical of degradation products (Fig. 4).

Northern blot analysis

To determine the polarity of the encapsidated viral RNA Northern blot analysis was carried out using strand-specific riboprobes complementary to the different RNA segments (Fig. 4). RNA molecules of both polarities appeared to be present in RNA isolated from purified virus preparations. Surprisingly, both polarities appear to be encapsidated in nearly equimolar amounts. This was confirmed in several Northern blot experiments. However, the hybridization signal obtained with probes recognizing (−)-polarity RNA was consistently slightly higher than that of (+)-stranded RNA, suggesting that the amount of (−)-RNA present in purified virus particles is a fraction higher than the amount of (+)-RNA. Hereafter, we use the terminology commonly used for negative- and ambisense viruses. The more abundant RNA will be referred to as viral RNA (vRNA), while the complementary RNA will be described as viral complementary (vc)RNA (Fig. 4). Numbering of the nucleotide positions will be indicated on the vRNA sequence.

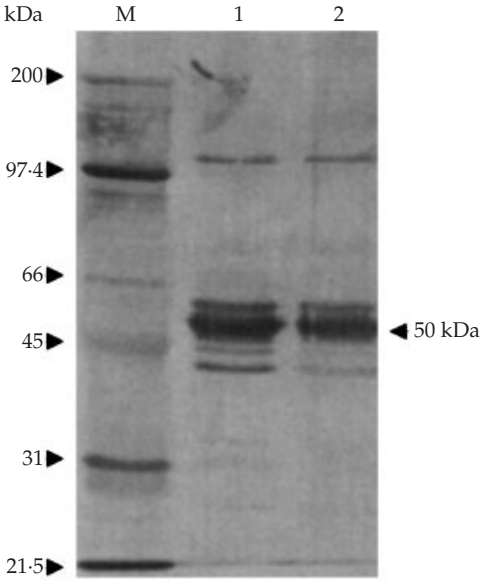

Fig. 1. Analysis of the MiLV structural proteins by SDS–PAGE. The proteins were visualized using a silver staining procedure. M, protein markers; lane 1 and 2, 0·1 and 0·5 μg of purified virus, respectively.

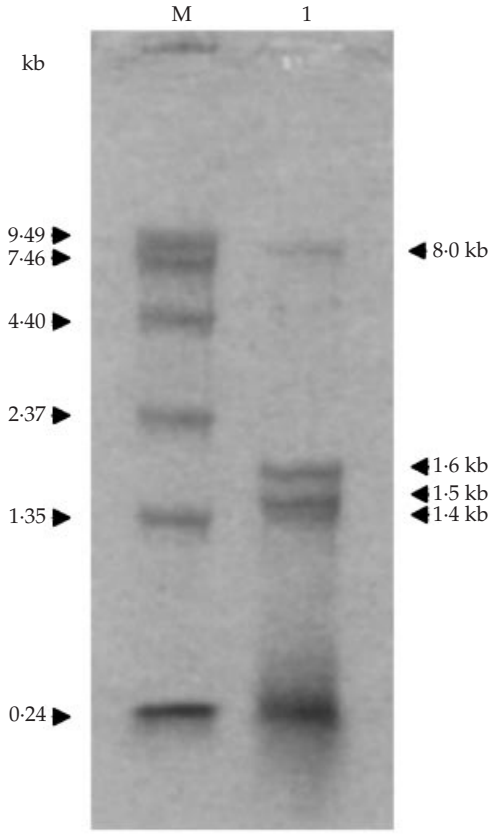

Fig. 2. Denaturing agarose gel electrophoresis. Sizes of the segments are indicated in kb. The gel was stained using *ortho*-toluidine blue. M, molecular size standard; lane 1, 2 μg of purified MiLV RNA.

Several other hybridization signals were observed on Northern blot, both smaller and larger in size than the genomic RNA segments (Fig. 4). The nature of these bands remains to be elucidated. Most likely, the smaller bands represent breakdown products while the larger RNAs possibly represent incompletely denatured RNA molecules.

Nucleotide sequence analysis

The complete nucleotide sequence of the genome of MiLV was elucidated by sequence determination of overlapping

A. Conserved terminal sequences

```
5'-ends
RNA1 5′ TGATATATTTTTAAAATATATTTTGATTAACTGAAACAAA.....
RNA2 5′ ------T----CT---A-----G-TG--G-ACCTT-A-TG.....
RNA3 5′ -----GT------TT-A-AC-A-CAGC-C--AT-CT-CCT.....
RNA4 5′ ------T------TT-A-A--A-CTG--C-ACTTTGTCTC.....

3'-ends
RNA1  .....TATTTCTTTTGAGAACTTGTTATATTTTTAAAAAATAATCa 3′
RNA2  .....-TG--GGGA---A----GT--TGCA-A-ATT---------- 3′
RNA3  .....-TG--T-C--AT--G------------------------- 3′
RNA4  .....CT---TCAC-AGAT-------TAT----------------- 3′
```

B. Putative panhandle structures

RNA1

```
5′ TGAT-ATATTTTTAAAATATATTTTGATTAACTGAAACAAACC.....
   |||| || |||| ||||||||    | ||  |  ||
3′ aCTAATAAAAAATTTTTATATTGTTC-AAGAGTTTTCTTTATA.....
```

RNA2

```
5′ TGAT-ATTTTTTC-TAAAAATATTGTTGTTGAACCTTAAATG.....
   |||| |||||    ||   | |    | || | ||  | |
3′ aCTAATAAAATTATATACGTTTTGTCAAAAGTAGGGTTGTTA.....
```

RNA3

```
5′ TGATAGTTTTTTATTAAAACTATCA-GCTCACATACTCCCTAT.....
   ||||  |||||||  |||  || || ||||| |      | |
3′ aCTAATAAAAAATT-TTTATATTGTTCGAGTATTCTTTTGTTG.....
```

RNA4

```
5′ TGATATTTTTTTATTAAAAATATCTGTTCAACTTTGTCTCAGT.....
   ||||  ||||| |  || ||       || | |
3′ aCTAATAAAAATTTTTTATTTGTTCATAGATCACTTTTTCCGT.....
```

C. Putative base-pairing structures according to the 'symmetrically hooked' model

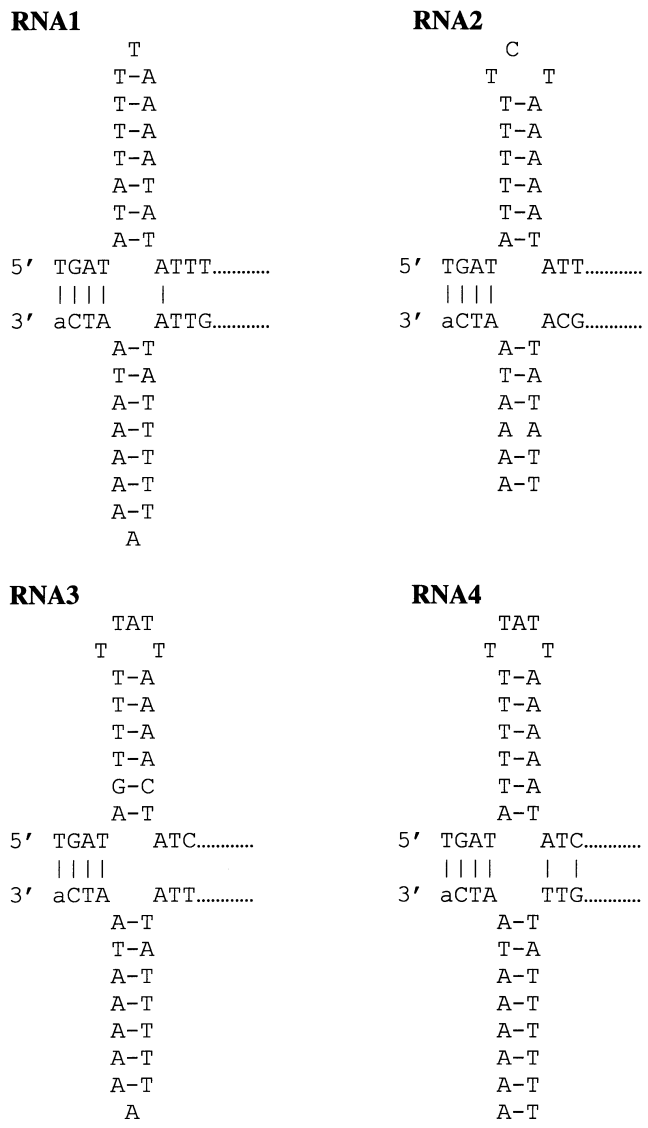

Fig. 3. (A) Alignment of the 3′ and 5′ ends of the different MiLV RNA segments. Identical nucleotides are indicated by dashes. The 3′-terminal A residue of the RNA segments has been indicated in lower-case, since the presence of this residue could not be unequivocally determined. (B) Putative panhandle structures formed by the 5′ and 3′ ends of the different MiLV RNA segments. (C) Putative base-pairing structures according to the 'symmetrically hooked' model.

cDNA clones. Northern blot analysis using total RNA isolated from infected and non-infected plant material confirmed that the cDNA clones obtained were virus specific (data not shown). Each nucleotide of the genome was determined unequivocally by sequencing of at least two different cDNA clones. The sequences of the extreme ends of the genomic RNAs were determined by amplification of the terminal sequences employing 5′ and 3′RACE procedures. The 5′ ends of the different vRNAs could be amplified using both a 5′RACE procedure and a 3′RACE procedure directed against the 3′ end of the vcRNAs, confirming that viral RNA molecules of both polarities were present in the purified virus preparations. On sequence analysis of the RACE clones obtained from the 5′ end of the vRNA segment 1 it was shown that the sequences obtained by the 3′RACE and the 5′RACE procedures were identical, suggesting that full-length complementary RNA acted as a template and not viral mRNA-like molecules.

Both the 5′ and 3′ ends are conserved among the different viral RNA segments (Fig. 3A). Because the 3′-terminal sequences of the different RNA segments were determined by the 3′RACE procedure it cannot be excluded that one or more

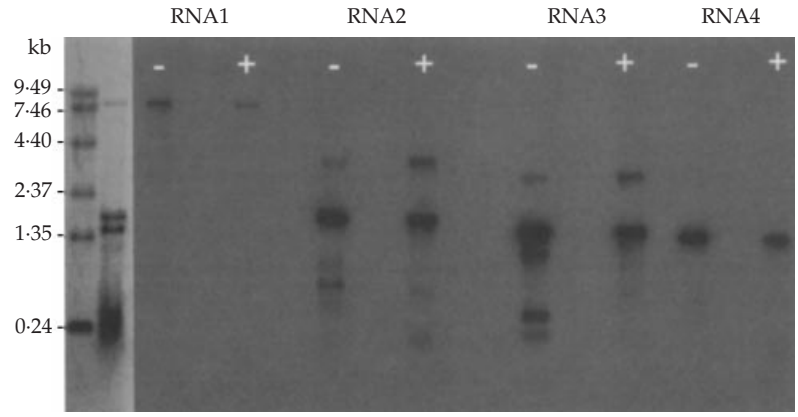

Fig. 4. Analysis of the RNAs isolated from purified virus particles by Northern blot hybridization using strand-specific digoxigenin-labelled riboprobes. 0·2 μg of viral RNA was used per lane. The probed segments and detected RNA strands (+ or −) are indicated above the lanes.

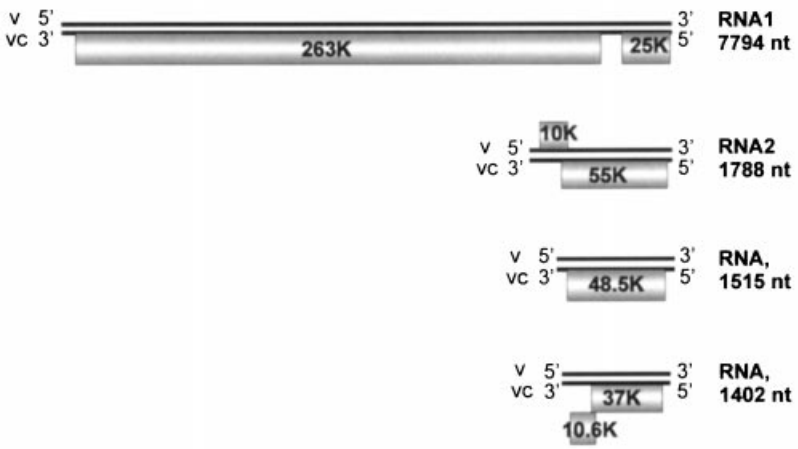

Fig. 5. Schematic representation of the genomic organization of the MiLV genome. Boxes represent ORFs. The length of the RNA segments and the predicted sizes of the ORF products are indicated. v, viral RNA; vc, viral complementary RNA

additional A residues are present at the 3′ ends of the RNAs. Analysis of the terminal sequences revealed that the 5′ and 3′ ends are, to a certain extent, inverted repeats which potentially can form panhandle structures (Fig. 3B). However, the 5′- and 3′-terminal sequences also contain palindromic sequences potentially able to fold into stem–loop structures (Fig. 3C).

ORFs

The MiLV RNA segment 1 is 7794 nt long and contains two ORFs on the vcRNA sequence (Fig. 5). The AUG start codon of the smallest ORF is located at position 7755 of the vRNA, and the ORF stops with an UAA stop codon at postion 7123. The putative ORF1 product is 24 776 Da ('25K' protein). The ORFs are separated by an intergenic region of 147 nucleotides. The large second ORF spans position 6976 (AUG start codon) to position 137 (UGA stop codon) of the vcRNA, encoding a protein of 262 635 Da (263K protein). To confirm that the presence of two ORFs on the RNA1 is a genomic feature conserved in other MiLV isolates, the sequence of the region spanning nucleotide position 6520–7273 (vRNA) was determined for a Norwegian isolate of lettuce big-vein disease-associated ophiovirus. This isolate has been in our collection since 1987. The sequence obtained was identical to that of the Dutch isolate, confirming that the presence of two ORFs is characteristic for the genomic organization of the virus and not typical of the Dutch isolate only.

The RNA segment 2 is 1788 nt in length. One major ORF is present on the vcRNA starting at position 1774 (of the vRNA) with an AUG start codon and terminating with an UAA stop codon at position 323, putatively encoding a protein of 483 amino acids with a molecular mass of 54 586 Da (55K protein). An additional minor ORF is present at the vRNA spanning position 126 (AUG) to 377 (UAG stop codon), putatively encoding a protein of 9960 Da (10K protein). The RNA3 is 1515 nt in length and contains one single large ORF at the vc strand. The vRNA does not encode ORFs of considerable length. The ORF commences at position (vRNA) 1428 and ends with an UGA stop codon at position 118, encoding a putative product of 48 544 Da (48·5K protein).

The vcRNA4 is 1402 nt in length and comprises two overlapping ORFs in different reading frames. The first ORF putatively encodes a protein of 37 261 Da (37K protein). The ORF starts with an AUG at position 1301 and ends at position 350 with an UGA stop codon. The second ORF overlaps the first ORF by 38 nucleotides, but appears to lack an initiation codon. This ORF has a theoretical coding capacity of 10 618 Da (10·6K) and starts at position 388 and continues to position 91.

To confirm that the observed frameshift in the reading frame was not caused by an artefact during the cloning procedure, the nucleotide sequence in this region was determined for two independent cDNA clones and three cloned RT–PCR fragments. Moreover, sequence analysis of this region in the RNA segment 4 of a Norwegian isolate confirmed the presence of a frameshift in the reading frame, thus ruling out the possibility that the observed frameshift was due to a mutation or presence of a defective RNA in the Dutch isolate. We suggest that the second ORF is expressed by a +1 translational frameshift. No structures like stem–loops or pseudoknots were detected in the putative frameshift region. However, a slippery sequence, GGGAAAU, known to be involved in −1 ribosomal frameshifting (Ten Dam *et al.*, 1990) can be recognized on the vc strand (position 1045–1052) immediately in front of the UGA stop codon of the 37K ORF.

Comparison of amino acid sequences

Comparison of the deduced amino acid sequences of the putative products of the ORFs located on the different RNA segments with sequences present in computer databases revealed that the 263K protein shared a high sequence similarity (72·5 %) with a partial sequence of the putative RNA-dependent RNA-polymerase (RdRp) of the ophiovirus *Ranunculus white mottle virus* (RWMV; AF335429). Moreover, the 263K protein showed low but significant amino acid sequence similarities with the L proteins of several rhabdoviruses [*Sonchus yellow net virus* (SYNV); *Rice transitory yellowing virus* (RTYV), *Viral haemorrhagic septicaemia virus* (VHSV), *Infectious haematopoietic necrosis virus* (IHNV); *Rabies virus* (RABV)]. No significant sequence similarities were detected in BLAST searches with the putative RdRps of bunyaviruses or tenuiviruses.

The 48·5K protein encoded by the RNA3 showed a high sequence similarity (44·6 %) with the coat protein of *Citrus psorosis virus* (Barthe *et al.*, 1998), indicating that the 48·5k protein is the MiLV coat protein or nucleocapsid protein. The deduced molecular mass of the putative nucleocapsid protein is consistent with the estimated size of the protein (Fig. 1). Database searches failed to detect proteins with significant sequence similarities with the other putative MiLV products.

Discussion

The complete nucleotide sequence of an ophiovirus, Miriafiori lettuce virus, associated with lettuce big-vein disease has been elucidated. Strikingly, the genome consisted of four RNA segments and not three molecules as previously reported for other ophioviruses. Northern blot analysis confirmed that the cloned RNA molecules were virus specific and revealed that both polarities of the genomic RNA were encapsidated in near equimolar amounts. Encapsidation of both polarities is a common feature among the *Tenuiviridae* and *Bunyaviridae*. However, in these viruses usually an excess of one polarity is encapsidated (Falk & Tsai, 1998). For the ophiovirus CPsV it has been reported that the negative-strand of the RNA3 was encapsidated in excess of the other polarity (de la Torre *et al.*, 1998). Possibly the presence of near equimolar amounts of both polarities in the virus particles is a characteristic feature of MiLV.

The genome of MiLV appears to be largely single-sense. All the ORFs were located on the vcRNA sequences, with the exception of the small 10K ORF located on the vRNA2 sequence (Fig. 5). It remains to be investigated whether the 10K ORF is functional and is expressed *in vivo*. The genomic organization of ophioviruses differs markedly from that of the tenuiviruses, which are ambisense.

Another unique feature of the MiLV genome is the presence of two overlapping reading frames on the RNA segment 4. The 10·6K ORF is possibly expressed by a +1 ribosomal frameshift, giving rise to a fusion protein containing both 37K and 10·6K sequences. The expression of viral genes by translational frameshifting is a common expression strategy observed in many virus genera. However, ribosomal frameshift usually involves expression of the −1 reading frame and not the +1 reading frame. One of the few examples of a +1 frameshift involves the expression of ORF1b of closteroviruses (Agranovsky, 1996; Rennecke & Jelkmann, 1998). Common secondary structures facilitating the +1 frameshift in the different closteroviruses have not been identified. (Fazelli & Rezaian, 2000; Melzer *et al.*, 2001). It has been suggested that the occurrence of a UUUC [*Grapevine leafroll-associated virus*-1 (GLRaV-1); GLRaV-3; Fazelli & Rezaian, 2000; *Pineapple mealybug wilt-associated virus*; Melzer *et al.*, 2001] or AAAG sequence (*Lettuce infectious yellows virus*; Klaassen *et al.*, 1995) in the overlap may cause frameshifting by slippage of $tRNA_{Phe}$ or $tRNA_{Lys}$, respectively. In the MiLV 10·6/37K ORF overlap the slippery heptanucleotide sequence GGGAAAU, known to be involved in −1 frameshifting (Ten Dam *et al.*, 1990), is present. Possibly by analogy to the above the GGGA sequence provides a slippery mechanism of $tRNA_{Gly}$ passage from one ORF to another.

It has been suggested that by analogy with the tenuiviruses the 5′ and 3′ end sequences of the ophiovirus RNA segments would be inverted repeats that can potentially form panhandle structures. Analysis of the MiLV terminal sequences revealed that the sequences are to a certain extent inverted repeats and that in contrast to the *Tenuiviridae* and *Bunyaviridae* the ends are not able to anneal to perfect panhandle structures. Furthermore, an absolute conservation of identical nucleotides at the genomic RNA termini as observed for the tenuiviruses and phleboviruses (family *Bunyaviridae*) appears to be absent in this ophiovirus. Interestingly, the terminal ends of the vRNA molecules of MiLV are able to anneal and fold into structures (Fig. 3C) faintly resembling the 'corkscrew' conformation of the RNA termini of the *Orthomyxoviridae* (Flick *et al.*, 1996). The influenza orthomyxovirus RNA promoter consists of the genomic 5′- and 3′-terminal sequences and is folded in a symmetrically hooked or 'corkscrew' conformation rather

A

Blast scores (bits)													
	MiLV	RWMV	IHNV	VHSV	RABV	SYNV	RTYV	RGSV	RHBV	RSV	RVFV	UUKV	TSWV
MiLV	5344	999	37		30	44	39			25			
RWMV	1006	1510				26	29				22		
IHNV	37		4700	600	50	56	49				23		
VHSV			598	4771	48	59	47					24	24
RABV	30		51	49	5141	97	89				23	24	25
SYNV	44	26	56	59	96	5145	256						
RTYV	39	29	49	49	89	256	4791	26		27		27	28
RGSV							26	7029	56	376	215	281	25
RHBV				22			23	55	1258	245	33	64	
RSV	25						27	376	247	6953	226	189	23
RVFV			23		23			217	34	228	5184	297	
UUKV				24	24		27	283	64	190	297	5108	
TSWV				24	25		28	25		23			6761

B

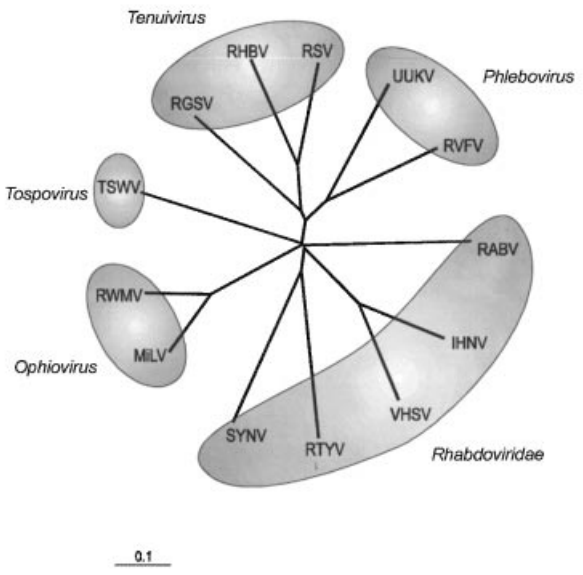

Fig. 6. (A) BLAST score table. Amino acid sequence comparisons using Blastp (Altschul *et al*., 1997) between the RdRps of the ophioviruses MiLV, RWMV (AF335429), the tenuiviruses *Rice grassy stunt virus* (RGSV; AB009656), *Rice stripe virus* (RSV; D31879), *Rice hoja blanca virus* (RHBV; AF009569), the phleboviruses *Rift valley fever virus* (RVFV; P27316), *Uukuniemi virus* (UUKV; P33453), the tospovirus *Tomato spotted wilt virus* (TSWV; P28976) and the rhabdoviruses RABV (P11213), SYNV (P31332), RTYV (AB011257), IHNV (L40883), VHSV (Y18263). Scores are indicated in bits, which represent the normalized scores derived from the raw alignment scores in which the statistical properties of the scoring system used have been taken into account. The raw scores of the alignments were calculated as the sum of substitution and gap scores (BLOSUM substitution scoring matrix). Non-significant scores are represented by blank boxes. (B) Phylogenetic analysis of the RdRps of the different viruses. Alignments were carried out using ClustalW (Thompson *et al*., 1994).

than a simple panhandle structure (Flick *et al*., 1996; Flick & Hobom, 1999). Interaction of the polymerase appears to be dependent on base-pairing according to the corkscrew model (Flick & Hobom, 1999). Possibly the ophiovirus promoter consists of a rather similar conformation.

The high degrees of similarities between corresponding tenuivirus and phlebovirus proteins, the similar genomic organization of these viruses, and sequence similarities between the termini of phleboviruses, nairoviruses and tenuiviruses have prompted the suggestion that viruses in the genera *Tenuivirus* and *Phlebovirus* have evolved from a common ancestor (Falk & Tsai, 1998). Based upon morphology and the presence of a segmented genome the ophioviruses appear related to the tenuiviruses. However, amino acid sequence comparisons of the MiLV RdRp sequence with the RdRp sequences of other negative-strand viruses revealed that rhabdoviruses are more closely related to MiLV and that the *Tenuivirus–Phlebovirus* cluster is more distantly related. No sequence similarities were observed between the other putative MiLV ORF products, like the nucleocapsid protein, and sequences in databases, including those of tenuiviruses. The observed sequence similarities between the different RdRps are low, and phylogenetic analysis based upon such data has to be interpreted with caution. However, a phylogenetic tree can be computed in close agreement with the results of Blastp (Altschul *et al*., 1997) alignments between the RdRps of the different viruses (Fig. 6A, B). This tree confirms the intergenic relationship between tenuiviruses and phleboviruses and shows that MiLV is closely related to RWMV but not to other viruses. These data suggest that from an evolutionary point of view ophioviruses are not closely linked to tenuiviruses.

The authors thank M. Fiers for his help with database searching and phylogenetic analysis. This work was supported by the European Commission under contract number QLRT-1999-01471.

References

Agranovsky, A. A. (1996). Principles of molecular organization, expression, and evolution of closteroviruses: over the barriers. *Advances in Virus Research* **47**, 119–158.

Altschul, S. F., Madden, T. L., Schaffer, A. A., Zhang, J., Zhang, Z., Miller, W. & Lipman, D. J. (1997). Gapped BLAST and PSI-BLAST: a new generation of protein database search programs. *Nucleic Acids Research* **25**, 3389–3402.

Barthe, G. A., Ceccardi, T. L., Manjunath, K. L. & Derrick, K. S. (1998). Citrus psorosis virus: nucleotide sequencing of the coat protein gene and detection by hybridization and RT–PCR. *Journal of General Virology* **79**, 1531–1537.

Campbell, R. N. (1962). Relationship between the lettuce big-vein virus and its vector, *Olpidium brassicae*. *Nature* **195**, 675–677.

De la Torre, S., Riva, O., Zandomeni, R., Grau, O. & Garcia, M. L. (1998). The top component of citrus psorosis virus contains two ssRNAs, the smaller encodes the coat protein. *Molecular Plant Pathology On-Line* http://www.bspp.org.uk/mppol/1998/1019sanchez.

Falk, B. W. & Tsai, J. H. (1998). Biology and molecular biology of viruses in the genus *Tenuivirus*. *Annual Review of Phytopathology* **36**, 139–163.

Fazelli, C. F. & Rezaian, M. A. (2000). Nucleotide sequence and organization of ten open reading frames in the genome of grapevine leafroll-associated virus 1 and identification of three subgenomic RNAs. *Journal of General Virology* **81**, 605–615.

Flick, R. & Hobom, G. (1999). Interaction of influenza virus polymerase with viral RNA in the 'corkscrew' conformation. *Journal of General Virology* **80**, 2565–2572.

Flick, R., Neumann, G., Hoffmann, E., Neumeier, E. & Hobom, G. (1996). Promoter elements in the influenza vRNA terminal structure. *RNA* **2**, 1046–1057.

Huijberts, N., Blystad, D.-R. & Bos, L. (1990). Lettuce big-vein virus: mechanical transmission and relationships to tobacco stunt virus. *Annals of Applied Biology* **116**, 463–475.

Klaassen, V. A., Boeshore, M. L., Koonin, E. V., Tian, T. & Falk, B. W. (1995). Genome structure and phylogenetic analysis of lettuce infectious yellows virus, a whitefly-transmitted, bipartite closterovirus. *Virology* **208**, 99–110.

Kuwata, S., Kubo, S., Yamashita, S. & Doi, Y. (1983). Rod-shaped particles, a probable entity of lettuce big-vein virus. *Annals of the Phytopathological Society of Japan* **49**, 246–251.

Laemmli, U. K. (1970). Cleavage of structural proteins during assembly of the head of bacteriophage T4. *Nature* **277**, 680–685.

Lot, H., Campbell, R. N., Souche, S., Milne, R. G. & Roggero, P. (2002). Transmission by *Olpidium brassicae* of Mirafiori lettuce virus and *Lettuce big-vein virus*, and their roles in lettuce big-vein etiology. *Phytopathology* **92**, 288–293.

Mayo, M. A. (2000). Genus *Varicosavirus*. In *Virus Taxonomy. Seventh Report of the International Committee on Taxonomy of Viruses*, pp. 521–523. Edited by M. H. V. van Regenmortel, C. M. Fauquet, D. H. L. Bishop, E. B. Carstens, M. K. Estes, S. M. Lemon, J. Maniloff, M. A. Mayo, D. J. McGeoch, C. R. Pringle & R. B. Wickner. San Diego: Academic Press.

Melzer, M. J., Karasev, A. V., Sether, D. M. & Hu, S. J. (2001). Nucleotide sequence, genome organization and phylogenetic analysis of pineapple mealybug wilt-associated virus-2. *Journal of General Virology* **82**, 1–7.

Milne, R. G., Garcia, M. L. & Grau, O. (2000). Genus *Ophiovirus*. In *Virus Taxonomy. Seventh Report of the International Committee on Taxonomy of Viruses*, pp. 627–631. Edited by M. H. V. van Regenmortel, C. M. Fauquet, D. H. L. Bishop, E. B. Carstens, M. K. Estes, S. M. Lemon, J. Maniloff, M. A. Mayo, D. J. McGeoch, C. R. Pringle & R. B. Wickner. San Diego: Academic Press.

Rennecke, B. & Jelkmann, W. (1998). Expression of the little cherry closterovirus RNA-polymerase by a +1 ribosomal frameshift. *Arbeitskreis Viruskrankheiten der Pflanzen*, November 12–13, Wageningen, The Netherlands.

Roggero, P., Ciuffo, M., Vaira, A. M., Accotto, G. P., Masenga, V. & Milne, R. G. (2000). An *Ophiovirus* isolated from lettuce with big-vein symptoms. *Archives of Virology* **145**, 2629–2642.

Roossinck, M. J. (1997). Mechanisms of plant virus evolution. *Annual Review of Phytopathology* **35**, 191–209.

Sambrook, J., Fritsch, E. F. & Maniatis, T. (1989). *Molecular Cloning: a Laboratory Manual*, 2nd edn. Cold Spring Harbor, NY: Cold Spring Harbor Laboratory.

Sasaya, T., Ishikawa, K. & Koganezawa, H. (2001). Nucleotide sequence of the coat protein gene of *Lettuce big-vein virus*. *Journal of General Virology* **82**, 1509–1515.

Ten Dam, E. B., Pleij, C. W. A. & Bosch, L. (1990). RNA pseudoknots:

translational frameshifting and readthrough on viral RNAs. *Virus Genes* **4**, 121–136.

Thompson, J. D., Higgins, D. G. & Gibson, T. J. (1994). CLUSTAL W: improving the sensitivity of progressive multiple sequence alignment through sequence weighting, positions-specific gap penalties and weight matrix choice. *Nucleic Acids Research* **22**, 4673–4680.

Vetten, H. J., Lesemann, D.-E. & Dalchow, J. (1987). Electron microscopical and serological detection of virus-like particles associated with lettuce big-vein disease. *Journal of Phytopathology* **120**, 53–59.

Received 23 May 2002; Accepted 9 July 2002